Yb-Doped Aluminophosphosilicate Triple-Clad Laser Fiber With High Efficiency and Excellent Laser Stability
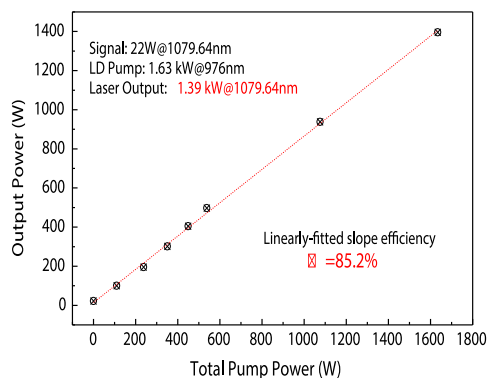
Shuang Liu
Huan Zhan
Kun Peng
Shihao Sun
Yuwei Li
Li Ni
Xiaolong Wang
Jiali Jiang
Juan Yu
Rihong Zhu
Jianjun Wang
Feng Jing
Aoxiang Lin

Signal: 22W@1079.64nm
LD Pump: 1.63 kW@976nm
Laser Output: 1.39 kW@1079.64nm

Linearly-fitted slope efficiency
⊗ =85.2%

Yb-Doped Aluminophosphosilicate Triple-Clad Laser Fiber With High Efficiency and Excellent Laser Stability

Shuang Liu [iD],[1],[2] **Huan Zhan,**[2] **Kun Peng,**[2] **Shihao Sun,**[2] **Yuwei Li** [iD],[2] **Li Ni,**[2] **Xiaolong Wang,**[2] **Jiali Jiang,**[2] **Juan Yu,**[2] **Rihong Zhu,**[1] **Jianjun Wang,**[2] **Feng Jing,**[2] **and Aoxiang Lin** [iD] [2]

[1]Advanced Launching Co-innovation Center, Nanjing University of Science and Technology, Nanjing 210094, China
[2]Laser Fusion Research Center, China Academy of Engineering Physics (CAEP), Mianyang 621900, China

Abstract: We fully demonstrated an ytterbium (Yb) doped triple-clad laser fiber with intense pump absorption, high efficiency, and laser stability. P^{5+}/Al^{3+} molar ratio in the central region of fiber core was specially designed to be ~1.08 for compensating P_2O_5 evaporation, while the ratio in the outer region was set as ~0.92 for obtaining a flattened refractive index profile. Applying a two-stage deposition process, one-time collapse technique, low-temperature multi-times sintering, and suitable flow of pure $POCl_3$ during sintering and collapsing process were instrumental in decreasing and offsetting element evaporation. Measured in an all-fiber master oscillator power amplifier configuration, the 7-m-long fiber obtained 1.39 kW near-single-mode laser output at 1079.6 nm with a slope efficiency of 85.2% and a beam quality M^2 of 1.36. Output laser spectrum with no sign of nonlinear-related peaks and a narrow 3-dB-bandwidth of ~0.33 nm was obtained. The fiber-based laser setup was kept at the maximum power for 1 h with power degradation less than 0.21%. The results demonstrated Yb-doped aluminophosphosilicate triple-clad fiber is a highly competitive candidate for commercial high-power laser and high-power narrow-linewidth fiber laser.

Index Terms: Fiber design and fabrication, lasers, fiber, fiber optics amplifiers and oscillators.

1. Introduction

Currently, mid-power (1~1.5 kW) ytterbium (Yb)-doped fiber (YDF) laser has taken the role as the next generation processing equipment [1]–[5]. The significant progress of mid-power industry fiber laser is known to be mainly contributed by the fast development of YDF and laser diodes (LDs) [1]–[3], [5]. To develop the multi-kW (≥2 kW) industry fiber laser, laser beam combining technology, especially incoherent beam combining, is a mainstream way in the current laser market [6]–[9]. However, laser beam quality is susceptible to the thermal distortion of the diffraction grating, the optical aberration of the transform lens, and the beam deviation of the laser arrays. Thus, it limits wide-use of this kind of laser, especially in precision mechanical processing [1]–[6]. A single

fiber laser is preferred because of diffraction-limited beams obtained in multi-kW regimes [1]–[9]. However, as the most key component in single-fiber lasers, YDF is easily subjected to undesirable limitation factor such as non-linear effects (e.g., stimulated Raman scattering (SRS)), excessive heating effect, and photodarkening (PD) effect [1]–[6]. The limit factors seriously impede long-term stability and durability for industry fiber laser working at multi-kW.

As the most widely-used YDF in industry fiber laser, large-mode-area double-clad fiber (LMA-DCF) consists of an Yb-doped core surrounded by a pure silica inner clad and a fluorine-doped polymer-based outer clad [4], [6], [10]–[14]. LMA-DCF has a relatively large core diameter of 20–30 μm to obtain multi-kW laser gain and low core numerical aperture (NA) for single-mode operation [4], [6], [10]–[14]. The fluorine-doped polymer-based clad is chosen as an outer clad for its low refractive index to enable pump light propagate within the inner clad [11], [13], [14]. Nufern Company (USA) successfully applies LMA-DCF into industry kW-level fiber laser products, working well on the market [1]–[6], [15]. Nevertheless, these polymer-based clad features low melting point and thermal damage threshold. So, it presents a significant challenge to industry fiber laser reliability [11], [13], [14]. As another promising YDF, metal coated optical fiber possesses a polymer-free all-glass optical fiber waveguide directly overcladed with a high thermal conductivity metal coating [11], [13], [16]. Such fiber was intensely investigated recently due to its intrinsic advantages including increased fiber operating ranges, reduction in peak core temperature, etc. [11], [13], [14]. Charles X. Yu *et al.* reported gold-coated specialty gain fibers [16]. This fiber presented 3.1 kW with 90% optical-to-optical efficiency and a beam quality M^2 of <1.15 [16]. However, the architectures of these reported metal-coated fiber laser were with separated free-space fiber components and individual optical devices, i.e., not an all-fiber laser system. In addition to this, it is a big challenge to stripe and recoat metal-clad fiber, fabricate metal-clad fiber-based components [11], [13], [14]. So, the metal-clad fiber laser is still unpractical for use out of laboratory up to now.

As an alternative to LMA-DCF, LMA triple-clad fiber (LMA-TCF) attracts more and more attentions recently since firstly fabricated and reported in [17]. The LMA-TCF was designed based on the LMA-DCF. The main difference with the conventional DCF is that there existed two glass-based clad next to the core region rather than one [17]–[20]. TCF shows obvious advantages over DCF with respect to laser-running stability and service life, as pump light rays were reflected by the second glass-based clad. This glass-based clad has a higher damage threshold and thermal-resistance ability than traditional polymer-based clad [18]–[20]. Nevertheless, these already-reported Yb-doped LMA-TCFs lasers [18]–[20] were only working at multi-hundred watt level because the host material is aluminosilicate (Al_2O_3-SiO_2, AS) glass and very difficult to obtain multi-kW laser output due to serious PD phenomenon [1]–[20]. On the other hand, LMA-TCF fiber proposed by Liekki Company (Finland) is commercially available [21], [22]. However, a rare report has publicly shown multi-kW laser output from commercial LMA-TCF. Preform fabrication technology and condition, especially rare-earths (REs) doping technique [22]–[29], is vital for high-quality LMA-TCF. Recently, organic chelate precursor doping technique (CPDT) has been proved effective to accomplish controllable and precise core deposition process with versatile refractive index profiles (RIPs) [24], [25], [27]–[31]. This technique enabled our research group to fabricate multi-kW nearly-PD-free aluminophosphosilicate (Al_2O_3-P_2O_5-SiO_2, ternary APS) laser fiber [24], [31], [32]. Nevertheless, the high sensitivity, low damage threshold polymer-based clad remains a limiting feature for the long-term (e.g., hundreds or thousands of hours) continuous operation of high power industry fiber lasers [13], [14], [16]. Our research group also made an Yb-doped APS (Yb-APS) TCF fiber by a combination of novel all-gas-phase CPDT, MCVD system, and a simple overcladding process [33]. However, the fiber presented obvious central dip, relatively high propagation loss of 32~36 dB/km at 1080 nm, and relatively serious elemental evaporation [33].

In this study, we reported on theoretical design, experimental fabrication, and laser performance of a kW-level Yb-APS TCF with high efficiency and low propagation loss of 25~27 dB/km at 1080 nm. Elemental evaporation was markedly compensated and improved by two-stage deposition, one-time collapse, low-temperature multi-times sintering, and suitable flow of pure POCl3 during sintering and collapsing process. Based on all-fiber master oscillator power amplifier (MOPA) configuration, the 7 m-long Yb-APS TCF showed 1.39 kW laser output at 1079.6 nm with an optical-to-optical

efficiency of 85.2% and a narrow 3 dB bandwidth of ∼0.33 nm. The results indicate the Yb-APS TCF is comparable to commercial Nufern-YDF-20/400-8 M fiber [25].

2. Experimental Details

2.1 Fiber Composition Design

For Yb-APS fiber, refractive index difference $\triangle n$ of the fiber core relative to undoped SiO_2 is determined by Yb^{3+} ions content, the molar ratio of Al and P, as well as Al and P content [27], [28], [31]. Aiming for high suppression of PD and low NA core, nearly equal content of Al and P was designed in the whole fiber core [24], [31], [32]. Considering extremely easy evaporation of P_2O_5 at the central region ($-5\ \mu$m $\leq$ r $\leq 5\ \mu$m, r is the radius), the molar ratio of P^{5+}/Al^{3+} in the region was specially designed to be a little over 1 for compensating P_2O_5 evaporation. So, it can suppress heterogeneity formation. Here, as total numbers of P is more than that of Al, the $\triangle n$ can be expressed as [27], [28], [31]:

$$\triangle n \cdot 10^4 = 67 c_{Yb_2O_3} + 15.2\left(c_{P_2O_5} - c_{Al_2O_3}\right) - 1.7 c_{Al_2O_3} \tag{1}$$

where $\triangle n$ is the refractive index difference compared to undoped SiO_2. $c_{Yb_2O_3}$, $c_{Al_2O_3}$ and $c_{P_2O_5}$ is the concentration of Yb_2O_3, Al_2O_3 and P_2O_5, respectively. For the outer region of the fiber core, P/Al molar ratio was designed to be a little less than 1 according to our previous report [31]. In this case, the $\triangle n$ can be obtained in the following equation [27], [28], [31]:

$$\triangle n \cdot 10^4 = 67 c_{Yb_2O_3} + 21.5\left(c_{Al_2O_3} - c_{P_2O_5}\right) - 1.7 c_{P_2O_5} \tag{2}$$

To improve pump absorption and offset evaporation loss, Yb^{3+} ions in the central region was increased to 0.2 mol%, while that of the outer region is set as 0.18 mol%. For the outer region, molar concentration of Al_2O_3 and P_2O_5 was 1.85 mol% and 1.7 mol%, respectively. The P^{5+}/Al^{3+} molar ratio is ∼0.92, and the NA was calculated to be ∼0.06 by Eq. 2. Compared with the outer region, the central region was designed to dope more P_2O_5 due to element evaporation. Moreover, to mitigate obvious fluctuation of $\triangle n$ and NA along the radial direction, the molar concentration of P_2O_5 and Al_2O_3 at the center region was set as 2.0 mol% and 1.85 mol%, respectively. It corresponds to the NA of 0.06 calculated by Eq. 1. The P^{5+}/Al^{3+} molar ratio is ∼1.08 in the central region of fiber core.

2.2 Fiber Fabrication and Characterization

The schematic diagrams of CPDT and MCVD used for preform fabrication were described in detail by our research group [24], [31]–[32]. Basically, experimental processes and procedures to make high quality Yb-APS TCF preform were almost in agreement with that reported in [33]. Different from that in [33], He gas flow rates in the last two deposition pass were increased to 225 sccm and 30 sccm for Yb and P, respectively. He gas flow rates for Al and Si were maintained at a constant during the whole core deposition process. Collapse passes were as many as 5∼7 in our previous work [24], [31]–[32]. To further decrease element evaporation, the ultra-thin substrate tube of ∼1 mm thickness was quickly collapsed against the gas flow direction, and collapse pass is as few as 1. We named the process as 'one-time collapse'. For our previous work [24], [31]–[32], a compact "mother preform" conventionally required sintering temperature of 2200∼2250 °C and sintering passes of 5∼7. In contrast, the sintering temperature was decreased to be 2000∼2050 °C so as to reduce element evaporation, and sintering passes were as many as 12∼15 for obtaining a compact preform, i.e., low-temperature multi-times sintering. Besides, suitable flow of pure POCl3 was maintained during sintering and collapsing process. It contributes to preventing the volatile phosphorus from evaporation [35]. The total length of the fabricated preform is ∼80 mm in order to shorten the collapse time and thus keep dopants survive into fiber core. The fluctuation of refractive index difference for the whole preform was controlled within 5% with a well-controlled CPDT process. Ultimately, the TCF preform was milled and drawn into a standard 20/400 μm fiber.
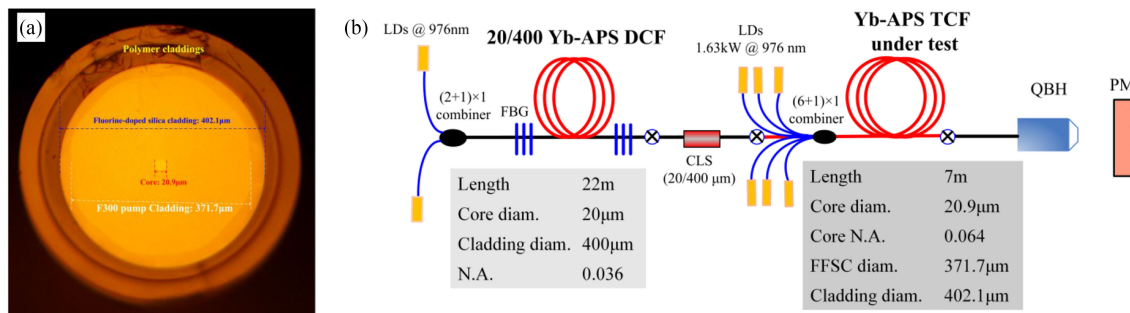
Fig. 1. (a) Cross section of the 20/400 Yb-APS TCF; (b) Schematic diagram of MOPA laser set-up. (LDs: laser diodes; FBG: fiber Bragg grating; CLS: cladding light stripper; QBH: quartz block holder; PM: power meter).

2.3 Fiber Structure and Laser Performance Measurements

As shown in Fig. 1(a), the drawn TCF has an Yb-APS core of 20.9 μm, an F300 pump clad of 371.7 μm, and an additional fluorine-doped fused silica clad (FFSC) of 402.1 μm, i.e., 20/400 Yb-APS TCF. Besides, the bare fiber was coated with a normal UV-curving low-refractive index polymer of ~485 μm and a high-refractive index polymer of ~550 μm. The fiber is with the same core-clad ratio to standard 20/400 μm LMA fiber [25], while core to pump-clad diameter ratio is calculated to be ~22.5/400. It contributes to high clad absorption of pump light. To investigate the continuous-wave (CW) laser performance of this Yb-APS TCF, we constructed an all-fiber master oscillator power amplifier (MOPA) configuration, as described in Fig. 1(b). The first oscillator stage is almost in accordance with that reported in [32]. Different from our previous work [32], core diameter of ultra-low NA fiber was decreased from 25 μm to 20 μm in order to match the pigtail fiber of cladding light stripper (CLS) and obtain near-diffraction limited laser beam. The seed light from the first oscillator stage is 22 W with a beam quality factor M^2 of 1.05 and a line-bandwidth of 0.26 nm. Total pump power of 1.63 kW was launched to F300-based inner clad by a (6 + 1) ×1 fiber combiner to realize power scaling. With 18 °C water-cooling, the Yb-APS TCF was deployed with coiling diameter of 300~400 mm on an aluminum cooling plate in order to avoid excessive pump bend-induced loss. The fiber laser beam was collimated and output by a Quartz Block Holder (QBH). Subsequently, it was split by beam splitters and attenuated to mW-level for spectrum and beam quality analysis. The output power stability was also recorded for further discussion.

3. Results and Discussion

3.1 Refractive Index Profile and Absorption Properties

Measured by the refracted near field method [24], [25], [31], [32], refractive index profile (RIP) of the fiber was given in Fig. 2. Different from the conventional DCF, the TCF has an additional rounded FFSC, which is easy to splice with commercial delivery fiber. The FFSC is characterized by a depressed refractive index, in the range of -21×10^{-3} with respect to F300 pump clad (see the Fig. 2(a)). It results in a pump NA of 0.206. As shown in Fig. 2(b), the core NA relative to F300 pump clad is ~0.064, corresponding to refractive index difference Δn of ~0.0014. Inconspicuous central-sunken in the fiber core can be observed. It validates the molar ratio design of P^{5+}/Al^{3+} along the radial direction of the fiber core. Meanwhile, it is believed to benefit good beam quality [36]. Clad absorption peak coefficients α at 915 nm and 976 nm were tested to be 0.63 dB/m and 2.06 dB/m (see the Fig. 3), respectively. As such, fiber length of 7 m was used here for TCF-based MOPA configuration. Benefiting from the TCF structure design, larger core-to-cladding ratio and higher Yb^{3+} ions concentration, pump absorption at 9xx nm studied here is more intense than that reported in [31]. So it is very beneficial to develop high-power narrow-linewidth fiber lasers for beam combination.
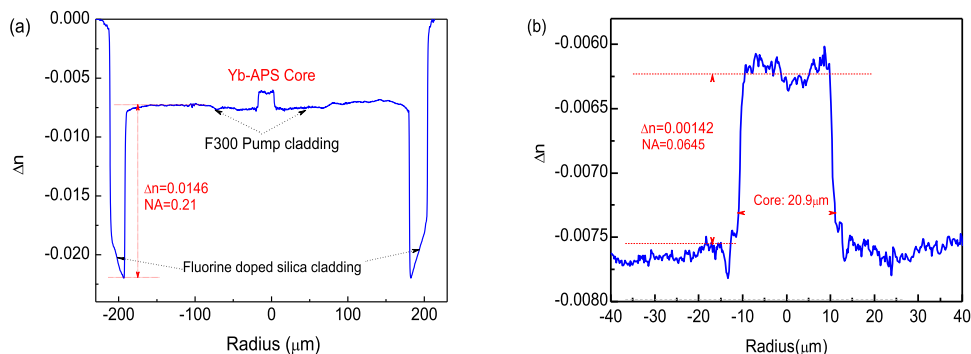
Fig. 2. Refractive index profile of (a) 20/400 μm Yb-APS TCF and (b) Yb-APS core.
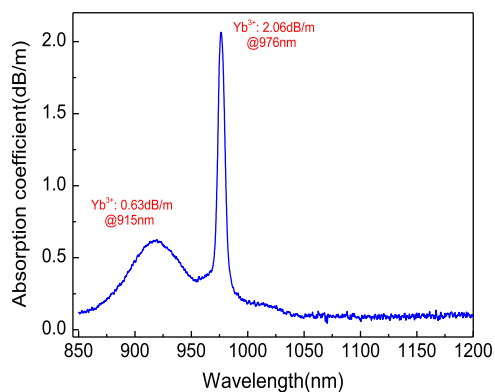

Fig. 3. Absorption spectrum of 20/400 μm Yb-APS TCF.

3.2 Rare-Earth Ions Distribution and Homogeneity

Elemental distribution was measured by an electron probe micro-analyzer (EPMA) [24], [25], [31]. Figure 4 presented the measured element distribution along the radial direction of the fiber core. For the outer region of the fiber core, molar percent of Yb_2O_3, Al_2O_3 and P_2O_5 was measured to be ~0.17 mol%, ~1.7 mol%, and ~1.6 mol%, respectively. Owing to the large $Yb(thd)_3$ and $POCl_3$ gas flow rates, the interface between the outer region and the central region was doped with ~0.19 mol% Yb_2O_3, ~1.75 mol% Al_2O_3, and ~1.82 mol% P_2O_5. Arising from elemental evaporation, the central region of the fiber core was doped with ~0.13 mol% Yb_2O_3, ~1.33 mol% Al_2O_3, and ~1.15 mol% P_2O_5, respectively (see the Fig. 4(a) and 4(b)). Nevertheless, the elemental loss in this study is much less than that reported in our previous work [33], [37]. The result indicates the methods including one-time collapse, low-temperature multi-times sintering and suitable flow of pure POCl3 during sintering and collapsing process are very effective to offset and decrease elemental evaporation. Recently, although Yb-APS fibers free from central dip of all elements were reported by D. S. Lipatov *et al.* [38] and M. Likhachev *et al.* [39], the low NA of 0.06~0.07 between the Yb-APS core and pump cladding is difficult to obtain due to high dopants concentration. In this case, the fiber-based laser systems has been constructed in a free-space structure due to the incompatibility of special low-NA fibers [39], and it has the disadvantage of massive volume and poor reliability. In the near future, by optimizing fabrication technique, for instance, further optimizing the temperature and He gas flow rates during the MCVD process, shortening preform length and applying small diameter substrate tube of 14 mm, central dips of Yb, Al and P element are possible to be mitigated. The RIP was calculated by Eq. 1 and Eq. 2 depending on the Al/P molar ratio. The result was shown in Fig. 4(c). The calculated RIP has almost no sunken in the central region. No obvious difference between the calculated and the measured RIP can be found. Nevertheless,
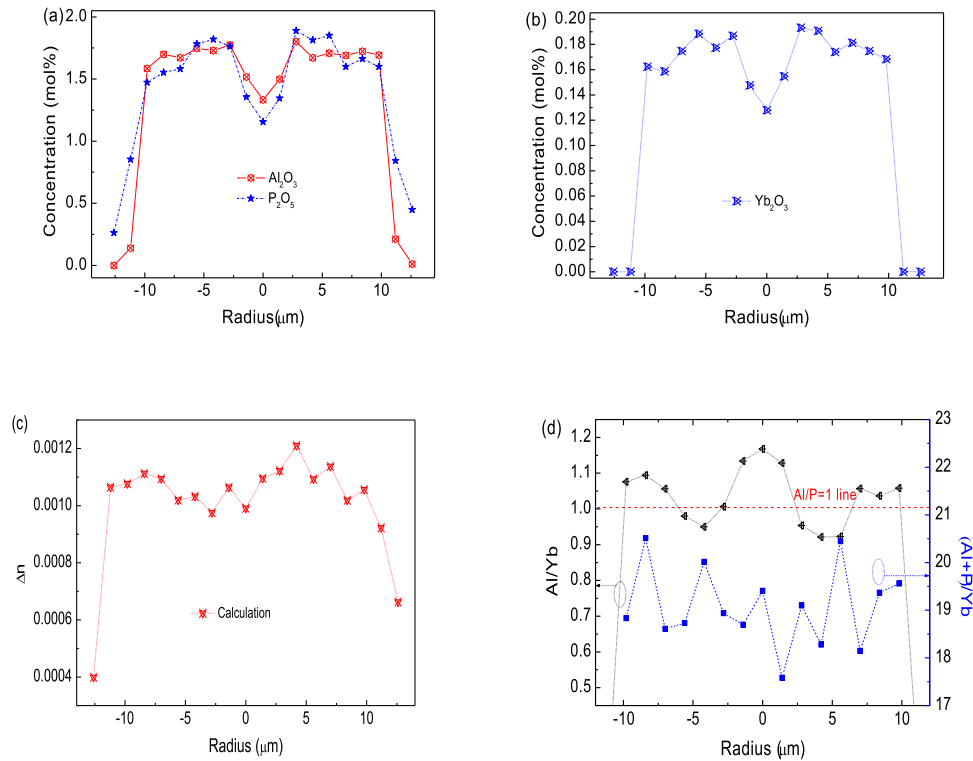
Fig. 4. Radial dopant concentration: (a) Al^{3+} and P^{5+} and (b) Yb^{3+}; (c) the calculated RIP of 20/400 Yb-APS TCF; (d) Al/P and (Al+P)/Yb ratio as a function of radius.

the experimentally measured $\triangle n$ value (see the Fig. 2b) becomes negative with respect to the calculated $\triangle n$ value. This is mainly originating from incomplete formation of $AlPO_4$ in the vicinity of Al:P = 1:1 [34], [35] and measure errors of the commercial devices. In addition to these, stresses and thermal treatment history influencing on refractive index in APS fiber were not considered here. The difference can be further shrunken by improving measure accuracy and introducing a fraction parameter f (which is a measure of the probability of $AlPO_4$ formation) in Eq. 1 and Eq. 2 as demonstrated in [35]. To examine the availability of the core composition design, Al/P and (Al+P)/Yb as a function of radius were calculated and presented in Fig. 4(d). In our previous work [31], (Al+P)/Yb molar ratio of the central region and the outer region is calculated to be 32 and 20, respectively. While, (Al+P)/Yb molar ratio of the central region is up to ~16.5, a little larger than that (18~20.5) of the outer region in this study. These results indirectly justified three measures, i.e., one-time collapse, low-temperature multi-times sintering and suitable flow of pure $POCl_3$ during sintering and collapsing process, were effective to reduce elemental evaporation. Besides, the large molar ratio makes Yb^{3+} ions homogeneously distribute and effectively prevent from clustering. As shown in Fig. 4(d), Al/P ratio in the whole fiber core was found to be ~1. Thus, it contributes to lower refractive index difference between core and clad. It is important to note Al/P ratio at the interface (between the central region and the outer region) is less than 1. To further verify the effectiveness of the two-stage deposition process, the element area distributions of Yb_2O_3, Al_2O_3 and P_2O_5 were characterized by EPMA with area analysis mode. The results were given in Fig. 5. It can be seen that the interface between the outer region and the central region presented higher element dopants concentration due to large $POCl_3$ and Yb (thd) $_3$ gas flow rates in the last two deposition pass during MCVD process. Even so, both the outer region and the central region showed a homogeneous elements distribution. It ensured low background loss in the whole fiber core in this study.
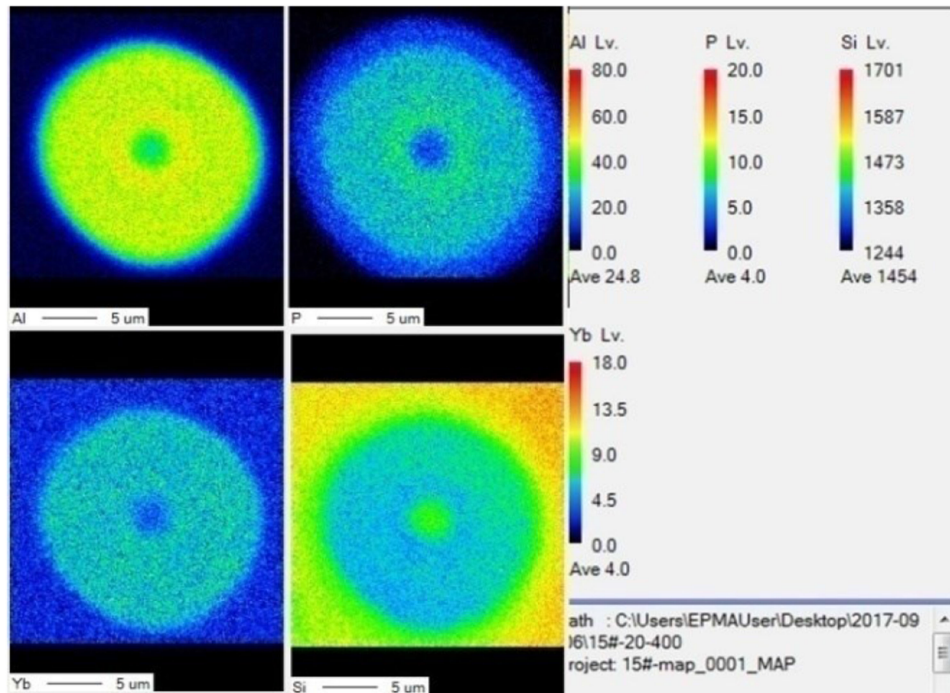
Fig. 5. (a) Al (b) P (c) Si (d) Yb distribution in the fiber core obtained by EPMA area analysis.
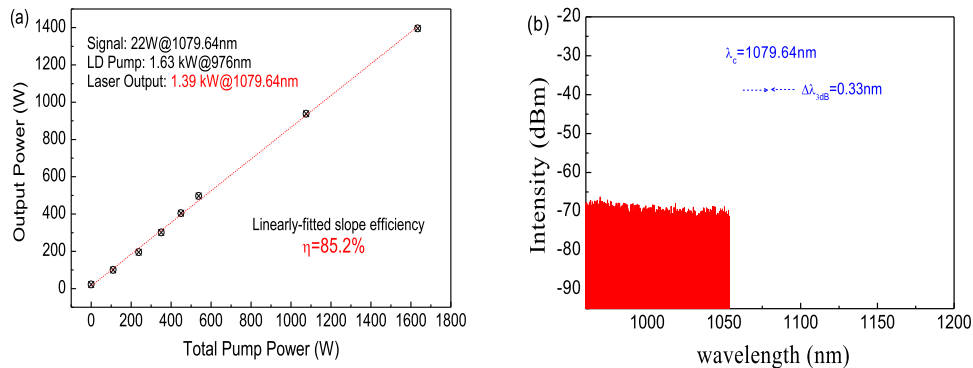

Fig. 6. Fiber laser experimental results of TCF fiber (a) Slope efficiency and (b) Laser output spectrum.

3.3 Laser Performance

Laser output power with respect to input pump power was measured in an all-fiber MOPA system with CPS component and shown in Fig. 6(a). The 7-m-long TCF was pumped up to an output power of 1.39 kW at 1079.6 nm. The linearly-fitted slope efficiency reached to 85.2%. The slope efficiency was calculated to be 84.3% at the highest pump power, comparable to that (84.9%) of LMA-YDF-20/400-8 M Yb-APS fiber [25]. It is well known quantum defect (QD) is the energy difference between pump and signal photons. It is converted to heat. The QD studied here can be calculated to be ∼9.54% according to the relationship reported in [40]. It is easy to conclude the slope efficiency with 84.3% is close to the theoretical limit. That is to say, the thermal load induced by the preparation technology can be neglected. As such, no thermal issue was observed in the whole laser setup. In our previous report [31], no CLS was used to dump the residual pump light and high-order modes propagating into the pump cladding. So the real slope efficiency is lower than the reported one. In contrast, with CLS, the whole laser setup studied here presented real slope efficiency as high as that reported in [31]. To our knowledge, this is the

(a)

Direct Power Stability Test at 1.36kW

Power Reduction<0.21%

(b)

M_x^2=1.32
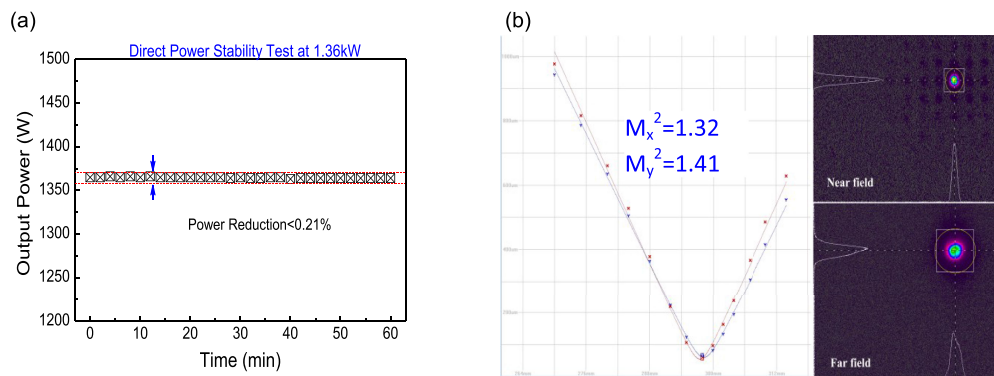M_y^2=1.41

Near field

Far field

Fig. 7. (a) Power stability test of laser systems setup at 1.36 kW; (b) Laser output beam quality at 1.39 kW.

highest slope efficiency value of the Yb-APS fiber publically reported by our group. The easily-fused splicing point between the combiner and the TCF was 22~23 °C. The polymer surface was recorded to be ~20 °C. The temperature rise should be induced by the mismatching between the TCF and the pigtail of the (6 + 1) × 1 combiner. Laser spectrum at 1.39 kW was shown in Fig. 6(b). The spectrum is centred at 1079.6 nm with a 3 dB bandwidth of ~0.33 nm. Benefiting from the short fiber length in use, no indication of SRS and amplified spontaneous emission was observed.

Aiming for investigating the laser stability of TCF, this MOPA laser setup was kept at ~1.36 kW for 60 minutes. As shown in Fig. 7(a), the output power presented a small power degradation of <0.21% lower than that reported in [25], [41], [42]. For our previous work [31], no CLS was used to dump the HOMs component and the residual pump. Thus, power degradation seems to be larger as compared with our earlier work [31]. However, owing to the imperfect splicing point and possible TMI in the 30 μm core [31], a few of HOMs component might propagate into the pump cladding. So, the 30/600 Yb-APS DCF-based laser setup with CLS [31] should present a small power degradation, which is possibly larger than that in this work. During this process, almost no temperature rise was found. Long-term power examination and further power scaling are limited by burn-in of (6 + 1) × 1 fiber combiner, and intended as our future work. Figure 7(b) presented the spatial beam quality of the constructed TCF-based amplifier in this study. The beam quality M^2 factor was measured to be ~1.36. It indicates that a near-single-mode laser output was obtained with our homemade Yb-APS TCF. In our earlier works [24], [31], the Yb-APS DCFs with 30 μm core might suffer from TMI and correspond to large M^2 factor above 2, which is not beneficial for beam combination. The good beam quality originates from low seed laser power with a M^2 of 1.05, short fiber length in use, low background loss of 25~27 dB/km at 1080 nm (25 dB/km at 1080 nm for Nufern-20/400-8 M fiber [25]), and good RIP as like that of commercial fiber [25]. The M^2 factor is larger than that of TCF-based oscillator case [33]. The worsening of beam quality is mainly induced by the excitation and amplification of the high-order modes. However, considering mismatching between TCF and other fiber components, slight beam quality degradation is relatively reasonable. Limited by the present experimental resources, mode instability (MI) could not be observed directly at the maximum power without high-speed camera or photodiode. It is well-known serious PD and MI phenomena lead to dynamical energy transfer between LP_{01} fundamental mode and HOMs [31], [43]. Some HOMs components are easy to leak into pump clad, and then stripped by the CPS. As a result, it comes along with the unstable beam profile in the fiber core as well as the degradation of laser power and optical-to-optical efficiency. As shown in Fig. 7(b), the beam profile at the maximum power is stable at both far-field and near-field. No serious distortion of the laser beam quality was found. Furthermore, no evidence of roll-over of output power or laser efficiency was observed when increasing pump power accordingly. The above-mentioned results and analysis indirectly ensure no obvious PD and MI phenomenon at the TCF-based laser system in this work.

4. Conclusions

In conclusion, we reported a kW-level Yb-doped triple-clad fiber fabricated by MCVD system, all-gas-phase chelate precursor doping technique, and a simple overcladding process. We applied one-time collapse, low-temperature multi-times sintering, a two-stage deposition process, and suitable flow of pure $POCl_3$ during sintering and collapsing process to effectively decrease and offset elements evaporation. With an all-fiber master oscillator power amplifier configuration, this fiber presented 1.39 kW laser output at 1079.6 nm with a high slope efficiency of 85.2% and an excellent beam factor M^2 of 1.36, i.e., a near-single-mode kW-level large-mode-area triple-clad fiber. Running of over 60 minutes at the maximum power presented power degradation less than 0.21%. Pure output spectrum with a narrow 3 dB linewidth of 0.33 nm was obtained. Future research work is potential to make the large-scale Yb-doped aluminophosphosilicate triple-clad fiber and develop high-power fiber laser toward 10 kW or above.

Acknowledgment

References

[1] D. A. Belforte, "A great year for the industrial laser business in the USA," *Laser Technik J.*, vol. 15, no. 2, pp. 30–31, 2018.

[2] G. Overton, A. Nogee, D. Belforte, and C. Holton, "Annual laser market review & forecast: Where have all the lasers gone?," *Laser Focus World*, vol. 53, pp. 1–24, 2017.

[3] http://www.ipgphotonics.com/index.htm

[4] C. Jauregui, J. Limpert, and A. Tűnnermann, "High-power fibre lasers," Nature Photon., vol. 7, pp. 861–867, 2013.

[5] I. P. G. Photonics, "IPG Photonics successfully tests world's first 10 kilowatt single-mode production laser," Jun. 15, 2009. [Online]. Available:http://www.ipgphotonics.com/newsproduct.htm

[6] C. Ye, L. Petit, J. J. Koponen, I. Hu, and A. Galvanauskas, "Short-term and long-term stability in ytterbium-doped high-power fiber lasers and amplifiers," *IEEE J. Sel. Topics Quantum Electron.*, vol. 20, no. 5, Sep./Oct. 2014, Art. no. 0903512.

[7] Y. Zheng *et al.*, "10.8 kW spectral beam combination of eight all-fiber superfluorescent sources and their dispersion compensation," *Opt. Exp.*, vol. 24, no. 11, pp. 12063–12071, 2016.

[8] F. Chen *et al.*, "10 kW-level spectral beam combination of two high power broad-linewidth fiber lasers by means of edge filters," *Opt. Exp.*, vol. 25, no. 26, pp. 32783–32791, 2017.

[9] C. Lei *et al.*, "Incoherent beam combining of fiber lasers by an all-fiber 7×1 signal combiner at a power level of 14 kW," *Opt. Exp.*, vol. 26, no. 7, pp. 10421–10427, 2018.

[10] M. N. Zervas and C. A. Codemard, "High power fiber lasers: A review," *IEEE J. Sel. Topics Quantum Electron.*, vol. 20, no. 5, Sep./Oct. 2014, Art. no. 0904123.

[11] K. Tankala, D. Guertin, J. Abramczyk, and N. Jacobson, "Reliability of low-index polymer coated double-clad fibers used in fiber lasers and amplifiers," *Opt. Eng.*, vol. 50, no. 11, 2011, Art. no. 111607.

[12] F. Beier *et al.*, "Single mode 4.3 kW output power from a diode-pumped Yb-doped fiber amplifier," *Opt. Exp.*, vol. 25, pp. 14892–14899, 2017.

[13] J. M. O. Daniel, N. Simakov, A. Hemming, W. A. Clarkson, and J. Haub, "Ultra-high temperature operation of atunable ytterbium fibre laser," in *Proc. Eur. Conf. Lasers Electro-Opt.*, 2015, Paper CJ_11_6.

[14] J. M. O. Daniel, N. Simakov, A. Hemming, W. A. Clarkson, and J. Haub, "Metal clad active fibres for power scaling and thermal management at kW power levels," *Opt. Exp.*, vol. 24, no. 16, pp. 18592–18606, 2017.

[15] A. Méndez and T. Morse, *Specialty Optical Fibers Handbook*. New York, NY, USA: Elsevier, 2011.

[16] C. X. Yu, O. Shatrovoy, T. Y. Fan, and T. F. Taunay, "Diode-pumped narrow linewidth multi-kilowatt metalized Yb fiber amplifier," *Opt. Lett.*, vol. 41, no. 22, pp. 5202–5205, 2016.

[17] J. R. Cozens and A. C. Boucouvalas, "Coaxial optical coupler," *Electron. Lett.*, vol. 18, pp. 138–140, 1982.

[18] P. Laperle, C. Paré, H. Zheng, and A. Croteau, "Yb-Doped LMA triple-clad fiber for power amplifiers," *Proc. SPIE*, vol. 6453, Feb. 21, 2007, Art. no. 645308.

[19] P. Laperle, C. Paré, H. Zheng, A. Croteau, and Y. Taillon, "Yb-doped LMA triple-clad fiber laser," *Proc. SPIE*, vol. 6343, Sep. 8, 2006, Art. no. 63430X.

[20] M. Leich *et al.*, "Highly efficient Yb-doped silica fibers prepared by power sinter technology," *Opt. Lett.*, vol. 36, pp. 1557–1559, 2011.

[21] http://www.nlight.net/

[22] M. E. Likhachev *et al.*, "Large-mode-area highly Yb-doped photodarkening-free Al_2O_3-P_2O_5-SiO_2-based fiber," in *Proc. Eur. Conf. Lasers Electro-Opt./EQEC*, Munich, Germany, May 22–26, 2011, Paper CJ_P24.

[23] A. Halder *et al.*, "Yb-doped large-mode-area Al-P-silicate laser fiber fabricated by MCVD," in *Proc. Conf. Lasers Electro-Opt.: Sci. Innov., (Opt. Soc. America)*, San Jose, CA, US, May 13–18, 2018, Paper JTh2A. 77.

[24] Y. Wang *et al.*, "30/900 Yb-doped aluminophosphosilicate fiber presenting 6.85 kW laser output pumped with commercial 976 nm laser diodes," *J. Lightw. Technol.*, vol. 36, no. 16, pp. 3396–3402, Aug. 2018.

[25] S. Sun *et al.*, "kW-level commercial Yb-doped aluminophosphosilicate ternary laser fiber," *Proc. SPIE*, vol. 10710, Mar. 5, 2018, Art. no. 107103F.

[26] S. Jetschke, S. Unger, A. Schwuchow, M. Leich, and J. Kirchhof, "Efficient Yb laser fibers with low photodarkening by optimization of the core composition," *Opt. Exp.*, vol. 16, no. 20, pp. 15540–15545, 2008.

[27] S. Unger, A. Schwuchow, J. Dellith, and J. Kirchhof, "Codoped materials for high power fiber lasers-diffusion behavior and optical properties," *Proc. SPIE*, vol. 6469, Feb. 20, 2007, Art. no. 646913.

[28] H. Zimer *et al.*, "Fibers and fiber-optic components for high-power fiber lasers," *Proc. SPIE*, vol. 7914, Feb. 10, 2011, Art. no. 791414.

[29] C. Hou *et al.*, "Optical properties of Yb-doped fibers prepared by gas phase doping," *Opt. Mater. Exp.*, vol. 6, no. 4, pp. 979–985, 2016.

[30] M. Saha, A. Pal, M. Pal, C. Guha, and R. Sen, "An optimized vapor phase doping process to fabricate large core Yb-doped fibers," *J. Lightw. Technol.*, vol. 33, no. 17, pp. 3533–541, Sep. 2015.

[31] S. Liu *et al.*, "Multi-kW Yb-doped aluminophosphosilicate fiber," *Opt. Mater. Exp.*, vol. 8, no. 8, pp. 2114–2124, 2018.

[32] K. Peng *et al.*, "Single-mode large-mode-area laser fiber with ultralow numerical aperture and high beam quality," *Appl. Opt.*, vol. 55, no. 35, pp. 10133–10137, 2016.

[33] S. Liu *et al.*, "Fabrication and laser performance of triple-clad Yb-doped aluminophosphosilicate fiber," *Opt. Fiber Technol.*, vol. 46, pp. 297–301, 2018.

[34] S. Kuhn *et al.*, "All-solution doping technique for high power fiber lasers-refractive index influence in the vicinity of Al:P = 1:1," in *Proc. Adv. Solid State Lasers, (Opt. Soc. America)*, Nagoya, Japan, Oct. 1–5, 2017, Paper ATu5A-6.

[35] S. Kuhn *et al.*, "Modelling the refractive index behavior of Al,P-doped SiO_2, fabricated by means of all-solution doping, in the vicinity of Al:P = 1:1," *Opt. Mater. Exp.*, vol. 8, no. 5, pp. 1328–1340, 2018.

[36] J. W. Dawson *et al.*, "Large flattened mode optical fiber for reduction of non-linear effects in optical fiber lasers," *Proc. SPIE*, vol. 5335, pp. 132–139, Jun. 7, 2004.

[37] C. Gao *et al.*, "Yb-doped aluminophosphosilicate laser fiber," *J. Lightw. Technol.*, vol. 34, no. 22, pp. 5170–5174, Nov. 2016.

[38] D. S. Lipatov, A. N. Guryanov, M. V. Yashkov, M. M. Bubnov, and M. E. Likhachevc, "Fabrication of Yb_2O_3-Al_2O_3-P_2O_5-SiO_2 optical fibers with a perfect step-Index profile by the MCVD process," *Inorganic Mater.*, vol. 54, no. 3, pp. 301–307, 2008.

[39] K. Bobkov *et al.*, "Sub-MW peak power diffraction-limited chirped-pulse monolithic Yb-doped tapered fiber amplifier," *Opt. Exp.*, vol. 25, pp. 26958–26972, 2017.

[40] T. Yao, J. Ji, and J. Nilsson, "Ultra-low quantum-defect heating in ytterbium-doped aluminosilicate fibers," *J. Lightw. Technol.*, vol. 32, no. 3, pp. 429–434, Feb. 2014.

[41] Y. Wang *et al.*, "Highly-stable 20/400 Yb-doped Large-mode-area Fiber with 3 kW Laser Output Power," in *Proc. Asia Commun. Photon. Conf. (Opt. Soc. America)*, Guang Zhou, China, Nov. 10–13, 2017, Paper M1A.3.

[42] Y. Li *et al.*, "Fiber design and fabrication of Yb/Ce co-doped aluminosilicate laser fiber with high laser stability," *Photon. J.*, vol. 10, no. 4, pp. 1–8, 2018.

[43] H. Otto *et al.*, "Temporal dynamics of mode instabilities in high-power fiber lasers and amplifiers," *Opt. Exp.*, vol. 20, pp. 15710–15722, 2012.